

A. Hieke
H.-D. Dörfler

Selected X-ray diffraction and differential scanning calorimetry investigations of the binary system K-palmitate/glycerol

Received: 14 April 1999
Accepted: 28 June 1999

A. Hieke · H.-D. Dörfler (✉)
TU Dresden, Institut für Physikalische
Chemie und Elektrochemie
Kolloidchemie, Mommsenstrasse 13
D-01062 Dresden, Germany

Abstract Three mole fractions of the binary system K-palmitate/glycerol (KC_{16}/Gl) $x_{\text{KC}_{16}} = 0.30, 0.37$ and 0.50 have been investigated as a function of temperature by small- and wide-angle X-ray diffraction investigations and differential scanning calorimetry (DSC) measurements. The existence of a gel-like region, named G_1 in the preliminary binary phase diagram [4], could not be confirmed. Consequently, a corrected version of the phase diagram of the KC_{16}/Gl system is established. According to this corrected phase diagram at low K-palmitate concentrations, $x_{\text{KC}_{16}} < 0.25$, the transitions crystalline phase (C) \leftrightarrow hexagonal phase, chains fluid (H_α) \leftrightarrow isotropic, micellar phase (S) occur with rising temperature. At $x_{\text{KC}_{16}} > 0.25$ the transitions

C \leftrightarrow gel phase (G) \leftrightarrow lamellar phase, chains fluid (L_α) were observed. X-ray diffraction and DSC measurements provided concordant results. Only differences in the phase transition temperatures from DSC curves obtained at rising and falling temperatures were observed. The phase transitions C \leftrightarrow G, G \leftrightarrow L_α and G \leftrightarrow H_α correlate with a sharp shift in the d value of the first small-angle reflection. The occurrence of the G phase is accompanied by a distinct split of the first small-angle reflections. Simultaneously, the wide-angle reflections change and the peak intensity is reduced.

Key words Nonaqueous lyotropic liquid crystals · X-ray diffraction · Calorimetry · Gel phase · K-palmitate · Phase diagram

Introduction

Our previously published X-ray diffraction investigations on K-soap/glycerol (Gl) systems [1–3] are continued with the K-palmitate (KC_{16})/Gl binary system. The investigations comprised samples with mole fractions $x_{\text{KC}_{16}} = 0.30, 0.37$ and 0.50 . The phase diagram published in 1993 [4] is shown in Fig 1a. The above-mentioned concentrations and the respective phase regions are marked. According to this phase diagram, based on polarized microscopy texture observations, a gel phase, G_1 , occurs between the lamellar phase, L_α , and the hexagonal phase, H_α , but we could not verify that this G_1 region resembles a unitary phase region; however, the combined X-ray diffraction and differential scanning calorimetry (DSC) measurements

reported in this paper clearly reveal the absence of this phase. The details of the method have already been given [1, 2].

Results

Investigations of the KC_{16}/Gl system at $x_{\text{KC}_{16}} = 0.30$

According to the phase diagram in Fig. 1a a phase sequence crystalline (C) \leftrightarrow G \leftrightarrow H_α occurs at $x_{\text{KC}_{16}} = 0.30$. The wide-angle diffractograms and the DSC data at rising temperature are displayed in Fig. 2. The DSC peak intensities of the phase transitions G \leftrightarrow H_α and $H_\alpha \leftrightarrow$ isotropic, micellar phase (S) are about 1 order of magnitude smaller than of the C \leftrightarrow G

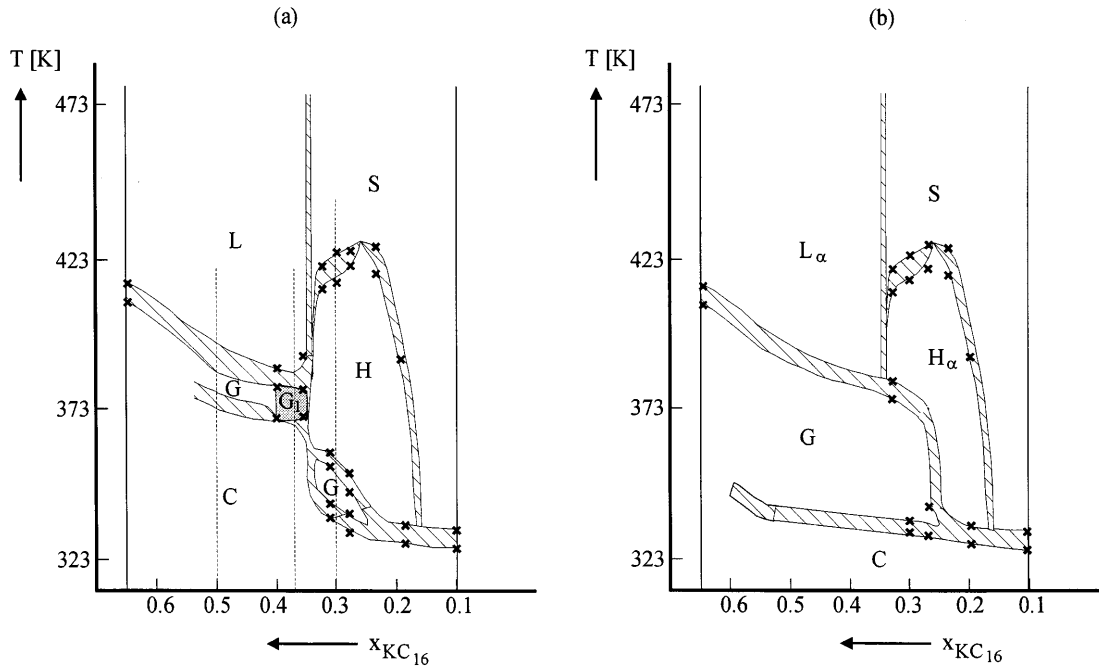


Fig. 1a, b Phase diagram of the K-palmitate/glycerol (KC_{16}/Gl) binary system. **a** Preliminary phase diagram based on texture observations [4]. **b** Revised phase diagram based on X-ray diffraction (XRD) and differential scanning calorimetry (DSC) measurements. The different phases are as follows: Crystalline phase (C), gel phase (G), hexagonal phase, chains fluid (H_α), lamellar phase, chains fluid (L_α), isotropic, micellar solution (S), second gel phase (G_1)

phase transition. Furthermore, a distinct regrouping and an intensity loss in the wide-angle X-ray diagram during the $C \leftrightarrow G$ phase transition are observed [2, 3]. The DSC curve shows a small pretransition at about 317 K. In this temperature range no corresponding modifications were found in the wide-angle X-ray diffractogram. Interestingly, the small-angle diffractograms (Fig. 3) reveal a broadened 001 reflection between the second and third curve. Furthermore, the amorphous background intensity increases slightly.

The observed characteristic small and wide-angle X-ray reflections clearly confirm the existence of a G region [2, 3]. According to the X-ray diffraction data and the DSC curve the H_α phase is formed at 373 K and is accompanied by the complete disappearance of the wide-angle reflections. Simultaneously, the intensity of the amorphous wide-angle background increases. Furthermore, the intensity of the first small-angle reflections increases at the transition into the H_α phase. As indicated in Fig. 3, the intensities of the 001 reflections are $I_{001} = 160$ cps at $T = 303$ K (C phase), $I_{001} = 760$ cps at $T = 393$ K (H_α phase) and $I_{001} = 80$ cps at $T = 423$ K (S phase). In agreement with the microscopic texture observations, the $H_\alpha \leftrightarrow S$ phase transition occurs at $T = 413$ K.

The d values (for a definition see Ref. [2]) of the first small-angle reflections and the DSC curves for heating and cooling are reported in Fig. 4. The $C \leftrightarrow G$ transition correlates with a sharp shift in the d value ($\Delta d \approx +0.30$ nm) of the small-angle 001 reflection. Within the H_α phase the d values decrease by $\Delta d \approx -0.05$ nm between $T = 373$ and 413 K but the intensity of the 001 reflection increases. Furthermore, the

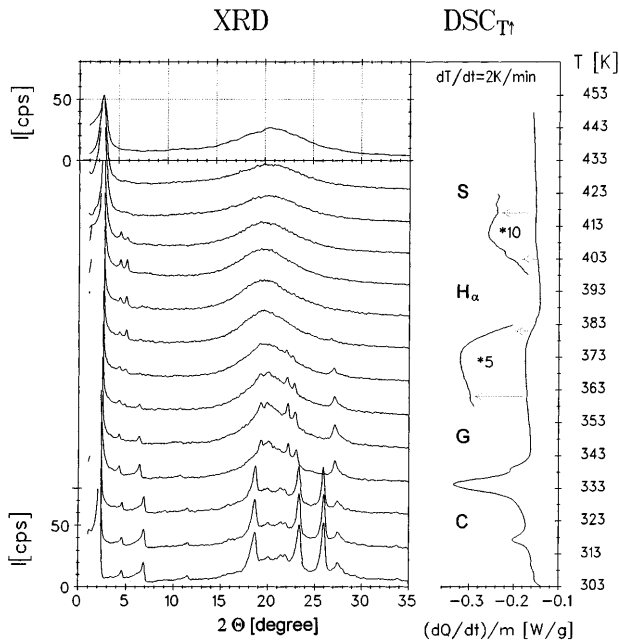


Fig. 2 Wide-angle X-ray diffractograms and DSC curve at rising temperature for KC_{16}/Gl at $x_{KC_{16}} = 0.30$

texture image from polarized microscopy becomes constantly sharper and more distinct.

Investigations of the KC_{16}/GI system at $x_{\text{KC}_{16}} = 0.37$

At this concentration the gel-like region, G_1 , which was found from our texture observations [4], should appear

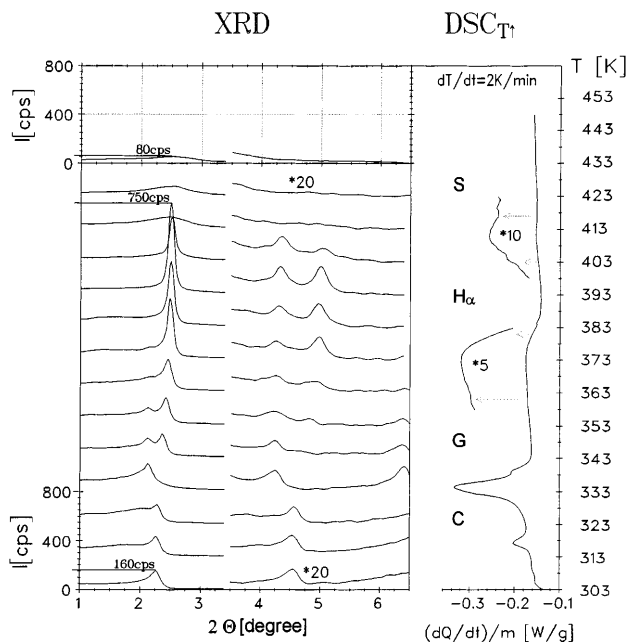


Fig. 3 Small-angle X-ray diffractograms and DSC curve at rising temperature for $(\text{KC}_{16}/\text{GI})$ at $x_{\text{KC}_{16}} = 0.30$

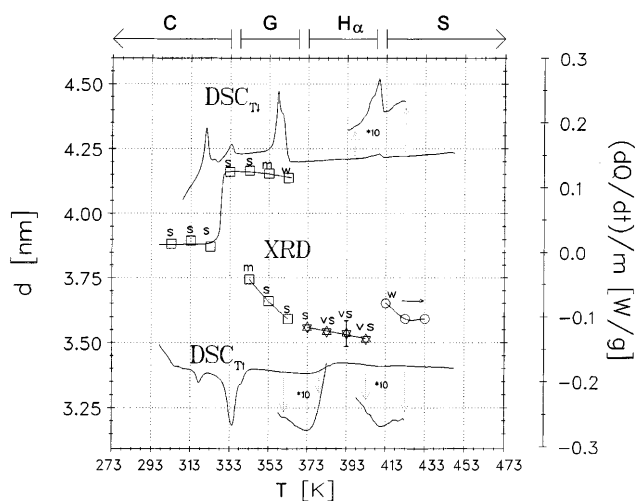


Fig. 4 d values of the first small-angle reflections and DSC curve at rising and falling temperatures for KC_{16}/GI at $x_{\text{KC}_{16}} = 0.30$. Reflections of the C and G phase \square , reflections of the H_α phase \star , reflections of the S phase \circ , Reflection intensity: weak (w), medium (m), strong (s), very strong (vs)

at rising temperature. In Fig. 5 the X-ray diffractograms and the DSC curve for rising temperature are shown. The $C \leftrightarrow G$ phase transition is clearly indicated at about $T \approx 338 \text{ K}$; however, this transition cannot be detected below $T \approx 363 \text{ K}$ by texture observations. Within the G phase the well-known characteristic small- and wide-angle reflections are found, and are comparable in position and intensity to those found in all other systems [5]. Again, the distinct split in the small-angle reflections is accompanied by weaker and rearranged wide-angle reflections with increased amorphous background. Consequently, the G_1 region in the preliminary binary phase diagram does not constitute a unitary phase region. The interpretation of our texture observation was wrong.

The small-angle X-ray diffractograms and the DSC curve for rising temperature (Fig. 6) allow the typical split of the small-angle reflections between $T = 343$ and 383 K to be recognized; this split is also evident from the second-order reflections. Consequently, the G phase extends further towards lower temperatures than initially assumed from the textures. Corresponding diffractograms have been found at $x_{\text{KC}_{16}} = 0.37$ and also at $x_{\text{KC}_{16}} = 0.50$ confirming a uniform, large G phase.

In Fig. 7 the d values of the first small-angle reflections with DSC curves obtained for rising and falling temperatures are compared. The $C \leftrightarrow G$ phase transition correlates with the characteristic split of the first small-angle reflection and a sharp shift in the d value of $\Delta d \approx +0.30 \text{ nm}$. Within the L_α phase the corresponding d values of about $d \approx 3.05 \text{ nm}$ are approximately $\Delta d \approx -0.80 \text{ nm}$ smaller than within the

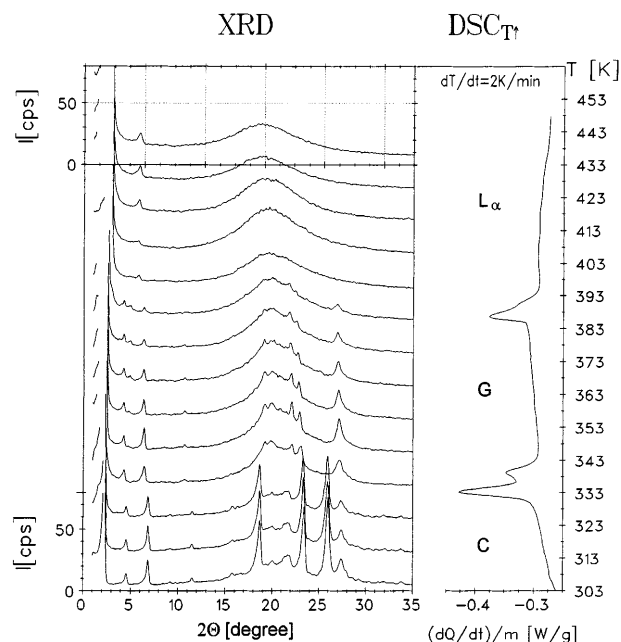


Fig. 5 Wide-angle X-ray diffractograms and DSC curve at rising temperature for $(\text{KC}_{16}/\text{GI})$ at $x_{\text{KC}_{16}} = 0.37$

C phase and decrease slightly by $\Delta d \approx -0.05$ nm in the temperature range between $T = 393$ and 433 K.

Investigations of the KC_{16}/Gl system at $x_{\text{KC}_{16}} = 0.50$

In this concentration region the phase-diagram shows the phase-transition sequence $C \leftrightarrow G \leftrightarrow L_\alpha$ (Fig. 8). Due to the high concentration of soap the transitions are relatively wide. The $C \leftrightarrow G$ transition occurs between $T = 323$ and 343 K. It is hardly possible to determine precisely the transition temperature from

texture observations. A value of $T \approx 368$ K was recorded based on texture observations. As mentioned, the diffractograms of the G phase are equivalent to those found at $x_{\text{KC}_{16}} = 0.37$. In agreement with the texture observations the $G \leftrightarrow L_\alpha$ transition was found between $T = 383$ and 393 K.

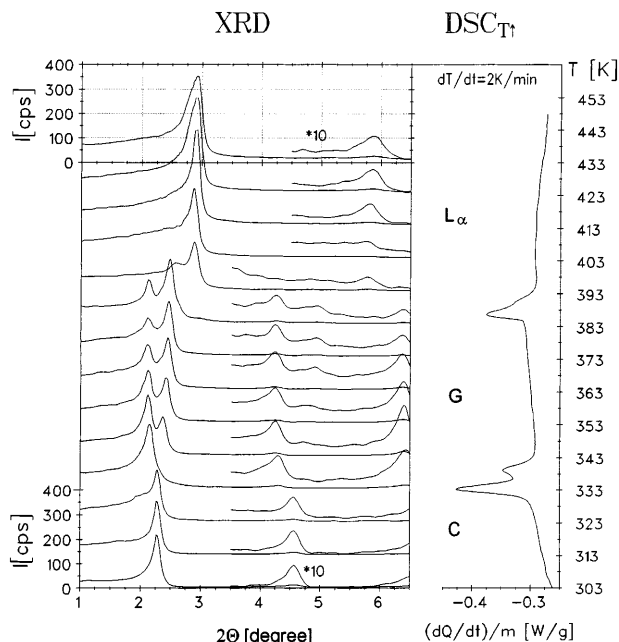


Fig. 6 Small-angle X-ray diffractograms and DSC curve at rising temperature for $(\text{KC}_{16}/\text{Gl})$ at $x_{\text{KC}_{16}} = 0.37$

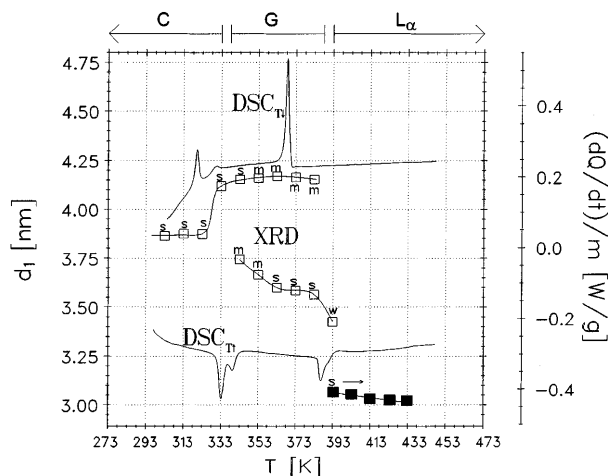


Fig. 7 d values of the first small-angle reflections and DSC curve at rising and falling temperatures for KC_{16}/Gl at $x_{\text{KC}_{16}} = 0.37$. Reflections of the L_α phase (■)

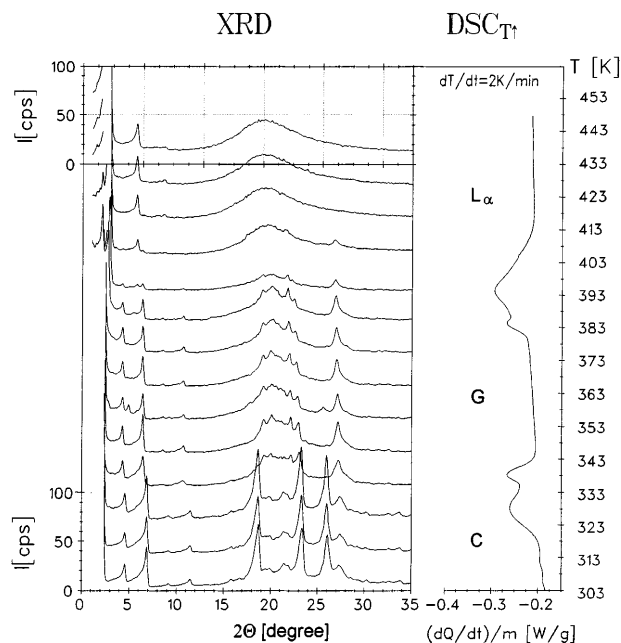


Fig. 8 Wide-angle X-ray diffractograms and DSC curve at rising temperature for KC_{16}/Gl at $x_{\text{KC}_{16}} = 0.50$

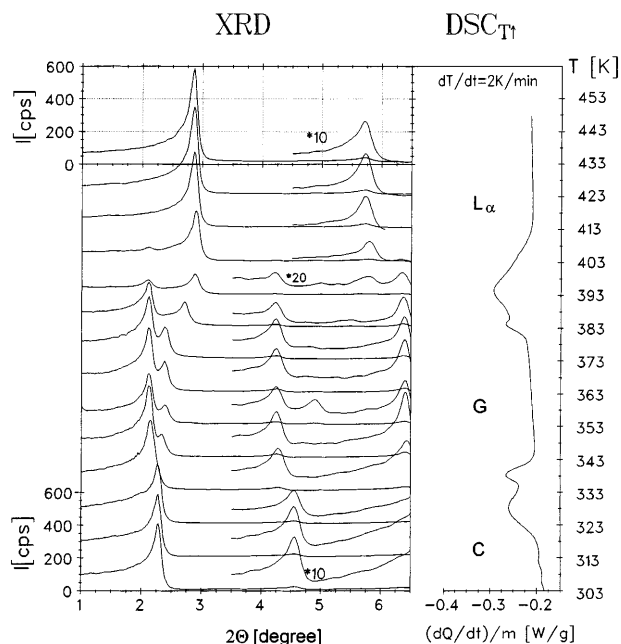


Fig. 9 Small-angle X-ray diffractograms and DSC curve at rising temperature for KC_{16}/Gl at $x_{\text{KC}_{16}} = 0.50$

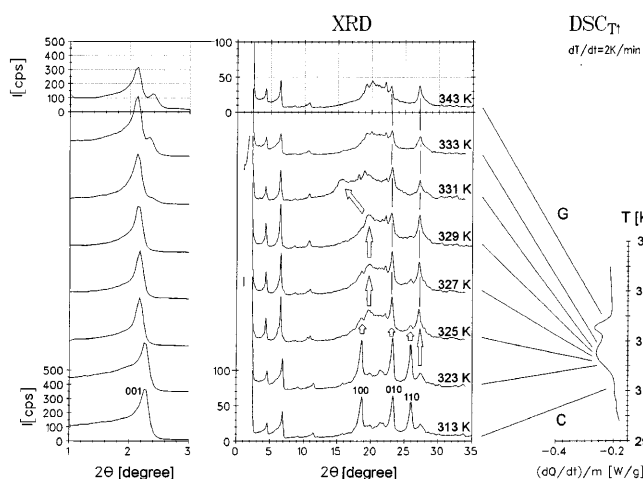


Fig. 10 Small- and wide-angle X-ray diffractograms and DSC curve at rising temperature throughout the C ↔ G phase transition for KC_{16}/Gl at $x_{\text{KC}_{16}} = 0.50$

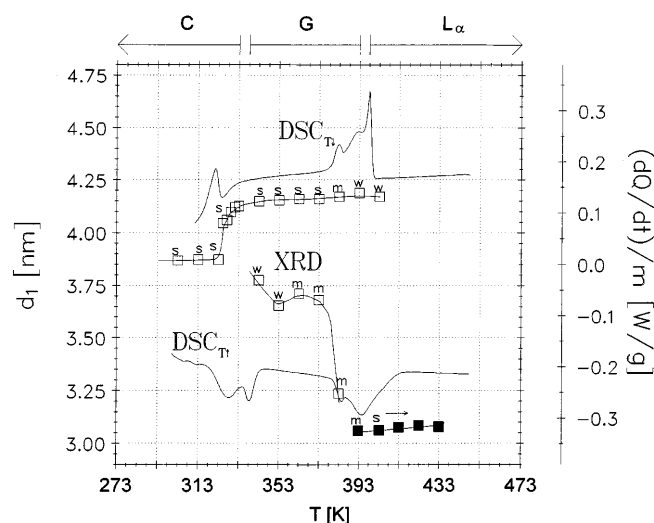


Fig. 11 d values of the first small-angle reflections and DSC curve at rising and falling temperatures for KC_{16}/Gl at $x_{\text{KC}_{16}} = 0.50$

In Fig. 9 the small-angle diffractograms and the DSC curve at rising temperature are compared. Within the G phase the known split of the 001 reflection occurs. The first peak, quasi still originating from the crystalline phase, disappears steadily. The second, new peak leads towards the position of the reflection present in the L_α phase. The formation of the L_α phase is complete at $T = 403$ K. The wide C ↔ G transition provided the

opportunity to study this phase transition in greater detail. For this purpose diffractograms were recorded in steps of $\Delta T = 2$ K between $T = 323$ and 333 K. The DSC curve of the phase transition and the diffractograms are shown in Fig. 10.

The sharp shift of the d value occurs between $T = 323$ and 325 K at the beginning of the transition and corresponds to an increased slope of the DSC curve: this is also seen in Fig. 11. The intensity of the 100 and 110 wide-angle reflections is reduced to approximately 10% compared to $T = 323$ K. The amorphous wide-angle background is enhanced and the broad reflection at $2\Theta = 27^\circ$, characteristic of the G phases, is established at $T = 325$ K. The d value of the 001 reflection increases only slightly between $T = 325$ and 329 K. Also, a broad wide-angle reflection at $2\Theta = 19.5^\circ$ becomes apparent, moving towards $2\Theta = 15.5^\circ$ between $T = 329$ and 331 K and is no longer observable at $T = 333$ K.

Considering X-ray diffraction measuring times of 8 h per temperature step it is reasonable to assume equilibrium states of the structural processes in the sample. Consequently, the DSC peak width is not primarily caused by the heating rate of $\Delta T/\Delta t = 2$ K/min, which may be considered to be too fast. Most likely, the phase transition occurs in two steps. First, the crystallographic order within the $[a, b]$ planes decreases corresponding to the reduced intensity of the wide-angle reflections. Also, the distance between the $[a, b]$ planes increases rapidly. The second step is the rearrangement of molecules within the $[a, b]$ planes as seen from the correlating regrouping of the weak wide-angle reflections. Finally, two different distances of the $[a, b]$ planes are preferred according to the distinct split of the first small-angle reflections. Throughout the whole phase transition only the 010 reflection can be traced unambiguously.

Conclusions

The X-ray diffraction and calorimetric measurements clearly indicate that the gel-like region, named G_1 (Fig. 1a) in the preliminary binary phase diagram [4], does not constitute a unitary phase region and is actually nonexistent. The corrected phase diagram is shown in Fig. 1b. The X-ray diffraction measurements and DSC investigations for $x_{\text{KC}_{16}} = 0.10$ and 0.25 reveal the polymorphism: $C \leftrightarrow H_\alpha \leftrightarrow S$. At $x_{\text{KC}_{16}} > 0.25$ the polymorphic $C \leftrightarrow G \leftrightarrow L_\alpha$ transitions were found.

References

- Hieke A, Dörfler HD (1999) Colloid Polym Sci 277: 494–498
- Hieke A, Dörfler HD (1999) Colloid Polym Sci 217: 762–776
- Hieke A, Dörfler HD (1999) Colloid Polym Sci 277: 777–784
- Dörfler HD, Senst A (1993) Colloid Polym Sci 271: 173–189
- Hieke A (1995) Thesis. TU Dresden